American Journal of Chemistry 2017, 7(5): 153-162
DOI: 10.5923/j.chemistry.20170705.01

Geochemical Characterization of the Black Shale from the Ama Fatma Coastal Site in the Southwest of Morocco

Samira El Aouidi[1,*], Said Fakhi[2], Abdelmourhit Laissaoui[1], Omar Ait Malek[3], Moncef Benmansour[1], Ayoub Ayach[2], Youness El Batal[3], Malika Aadjour[3], Mounia Tahri[1], Adil El Yahyaoui[1], Azouz Benkdad[1]

[1]Centre National de l'Energie, des Sciences et des Techniques Nucléaires (CNESTEN), Rabat, Morocco
[2]Hassan II University of Casablanca, Engineering and Materials Laboratory (LIMA), Thermostructural Materials, Polymers and Radiochemistry Team (TMPR), Faculty of Sciences Ben M'Sik Casablanca, Morocco
[3]Hassan II University of Casablanca, Geodynamics of Old Chains Laboratory, Faculty of Sciences Ben M'Sik Casablanca, Morocco

Abstract Application of natural geological materials as traps of stable and radioactive metals is part of the overall Moroccan vision for the treatment of radioactive wastes. In this context, the present work focuses on the geochemical characterization of a series of natural black shale samples collected for the Ama Fatma coastal site located in the Moroccan basin of Tarfaya-Boujdour. Major and trace elements were determined by using X-Ray fluorescence and Inductively Coupled Plasma – Mass Spectrometry (ICP-MS). Among the major elements determined, CaO was the most abundant component followed by silicon and iron oxides. Comparison between the obtained results and the geochemical standards indicated that Al, K, Ti, Mg were present in similar concentrations, Ca, Fe, P, and Mg were higher while Si was much lower. The mineralogical composition, determined by X-ray diffraction, showed that the samples were composed essentially of calcite (up to 70%). The predominance of carbonates in the sedimentary environment revealed that the deposition occurred in open marine settings. On the other hand, correlation analysis was carried out in an attempt to establish the elements association and origin, while element ratios were used as indicators of redox conditions, suggesting that the black shale were deposited during anoxic conditions.

Keywords Black shale, Ama Fatma, Morocco, Major and trace elements, Mineralogy, Enrichment factor, Redox reconstruction

1. Introduction

Shale rocks are sedimentary formations which belong to the category of mudstones because they result from the compaction of mud mineral particles over very large timescales. During the last decades, and besides being a potential source of non-conventional hydrocarbons (Dyni and Qian 2006), black shalerocks have been explored to prove their suitability as geological media for long term radioactive waste disposal (Frank et al. 2010; Christopher 2014). Indeed, their specific properties such as low permeability, self-sealing, the prevailing chemically reducing conditions and their high capacity of sorption make the shale formations ideal candidates to permanently host high level radioactive wastes repositories.

Morocco has three major black shale deposits, namely Tanger, Tarfaya and Timahdit belonging to the Upper Cretaceous, 70 Myrs, which represent about 15% of known black shale reserves in the world (Ambles et al. 1988). Many studies have been carried on these black shale, among them chemical characterization of kerogen (Ambles et al. 1988) and composition and physicochemical properties (Saoiabi et al. 2001). The main chemical studies concerning the black shale from Timahdit involved its pyrolysis (Nuttall et al. 1983) and its thermal degradation (Alaoui-Sosse et al. 1988). On the other hand, black shale from the Tarfaya basin were explored for their geochemical characterization (Kolonica et al. 2002), and the work was aimed at producing new adsorbents and testing them for their potential in trapping of radionuclides such as U and Th isotopes (Bekri et al. 1991; Khouya et al. 2002; Galindo et al. 2007). The Ama Fatma is located in the basin of Tarfaya-Boujdour. The basin corresponds to the section of the Atlantic margin between the town of Tarfaya in the north and that of Boujdour in the south. It is limited in the west by the Atlantic Ocean and in the east by the Republic of Mauritania (Figure 1). This area is located on the road leading to Tarfaya, about 80 km north of the city. This section begins with black shale thicker than 2 m (Figure 2) (El Batal 2014), alternating with grayish to blackish limestones, The Ama Fatma cut has been dated thanks to numerous ammonites, it is of lower Turonian age.

* Corresponding author:
elaouidi.samira@hotmail.fr (Samira El Aouidi)
Published online at http://journal.sapub.org/chemistry

The black shale of Ama Fatma, which is the subject of the present study, has been found to be rich enough of organic matter chemically linked to a mineral matrix (Khouya 2002). Organic deposits were previously interpreted as the result of early coastal upwellings (Einsele and Wiedmann 1982).

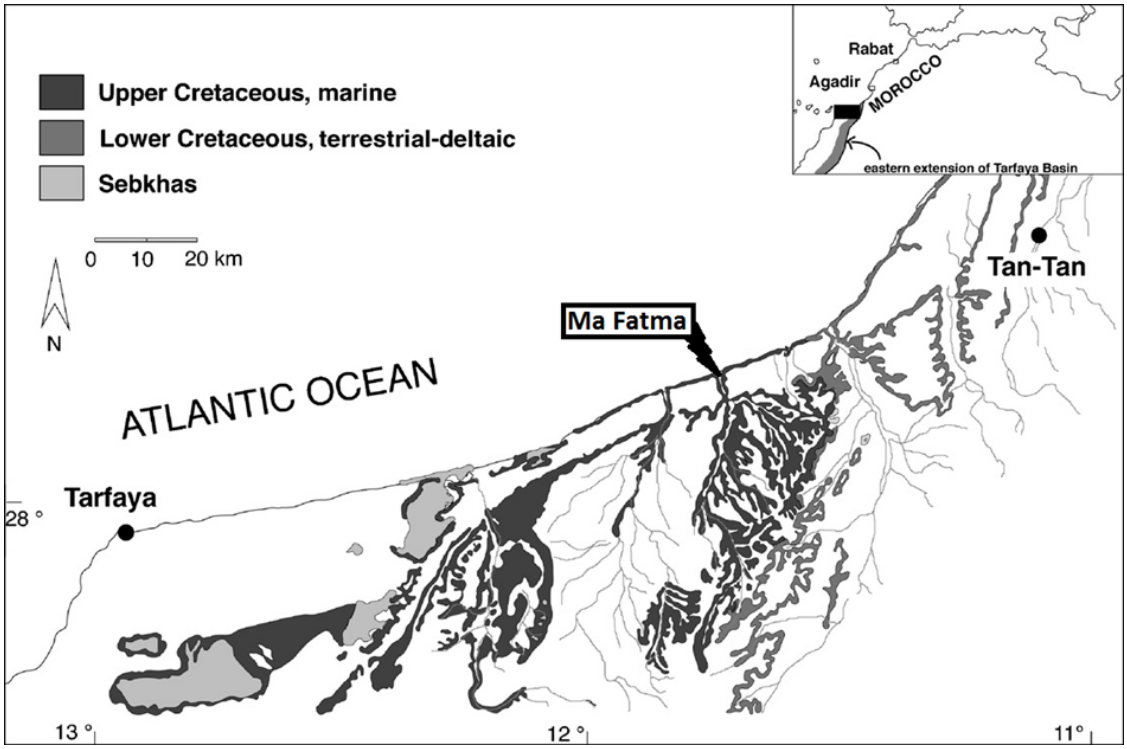

Figure 1. A sketched map of the study area showing its main geological features (Gebhardt and Zorn 2008)

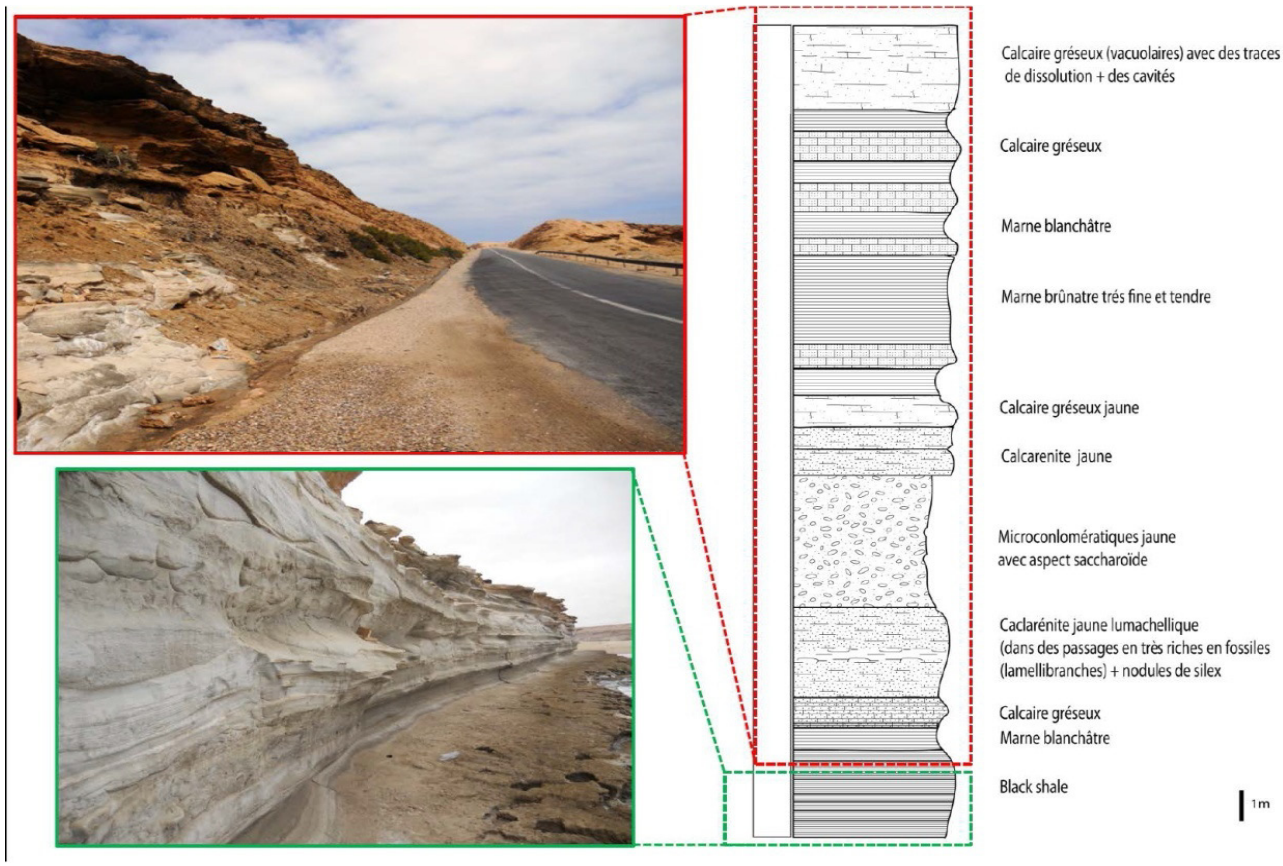

Figure 2. Pictures and schematic profile showing the stratigraphic layers of the studied location (El Batal 2014)

In the framework of the research being carried out on natural matrices for the long storage of radioactive wastes, the main objective of this study was to characterize the rock shale samples, collected from the Ama Fatma location belonging to the Tarfaya bassin, form a mineralogical and chemical point of view. This included the mineralogical composition, major element geochemistry, trace elements enrichment and their subsequent use in redox conditions reconstruction.

2. Material and Methods

2.1. Characterization

Prior to characterization and geochemical analyses, the collected black shale samples (El Batal 2014) were ground to fine powder using electric grinder. The mineralogy of the samples was determined in the National Center of Scientific and Technical Research (CNRST) by X-ray diffractometry using The X'Pert Pro MPD PAnalytical 2-circle diffractometer installed equipped with a thêta-thêta goniometer, a rapid X'Celerator detector, a sample changer and a high temperature chamber. Particle size distributions were determined in the National Center for Energy Sciences and Nuclear Techniques (CNESTEN- Morocco) in the homogenized sub-samples using a wet Laser Diffraction equipment (Malvern Mastersizer 2000) using the Hydro 2000G dispersion Unit. The particle size distribution range is 0.02–2000 µm. A small amount of sample (1g) was introduced in the dispersion unit containing demineralized water, used as dispersant, and then measured after a brief time (10s) of ultrasound application to disperse any agglomerates.

2.2. Determination of Major and Traces Elements

Major elements data were obtained by using X-ray fluorescence (XRF) S1 Turbo SD spectrometer. For trace elements determination, 50 mg of the fine fraction of each sample was weighed into acid-cleaned Teflon vessels, and 3 ml of HNO_3 Supra pure and 5 ml of HF were added. The mixture was allowed to react overnight and then subjected to microwave digestion Speed Wave Four (Berghof technologies). The obtained solubilized samples were analyzed by ICP-MS using a Thermo Scientific XSERIES 2.

3. Results and Discussion

3.1. Black Shale Characterization

From Table 1, the granulometric distribution showed a predominance of sand (50.42 – 83.76%), followed by silt (16.13 – 30.18%) and then clays with contents ranging from 0.1% to 19.40% with the highest value recorded at the upper layer, S1(9). Consequently, the black shale samples, subject of this study, have predominantly a sandy loam texture.

In Table 1, the mineralogical composition, obtained by X-ray diffraction analysis, is given. Calcite is the major constituent of the black shale of the Ama Fatma site. The percentages of calcite were ranging from 47.9 to 70.2%, while other minerals such as dolomite (4.7 à 20.6%), Quartz (3.4 à 17.5%), clays (3.7 – 8.3%), halite (2.7 – 7.3%), fluorapatite (0.4 – 13.3%) and pyrite (0.3 – 9.7%) were relatively less abundant.

Table 1. Particle size and mineralogical composition of the black shale from the Ama Fatma site.TOC contents were determined by El Batal (2014)

feature/Samples		S1(9)	S1(10)	S1(10-13)	S1(13-14)	S1(14)	S1(15)	S1(16)
TOC (%)		6.19	5.84	5.84	5.84	5.91	-	7.64
Depth (m)		24.18	24.69	24.83	24.95	25.27	25.8	26.69
Particle size	Clay	19.4	0.31	0.33	0.1	5.34	0.23	0.21
	Silt	30.18	19.27	24.77	16.13	27.25	26.33	23.79
	Sand	50.42	80.43	54.17	83.76	67.41	73.45	75.99
Mineralogy	Calcite	70.2	65.3	55.8	67.6	66.9	47.9	65.1
	Dolomite	8.6	8.8	14.4	4.7	4.8	20.6	14.8
	Quartz	6.8	7.3	17.5	3.4	6.7	17.2	8.4
	Clay	5.5	4.7	7.4	3.7	3.9	8.1	8.3
	Halite	7.3	3.1	4.4	5.7	2.7	4.1	3.3
	Fluorapatite	1.6	9.4	0.4	13.3	5.4	0.4	-
	Pyrite	-	1.5	0.3	1.7	9.7	1.6	-

Table 1. Concentrations of major elements in the black shale from the Ama Fatma site along with the corresponding averaged values in UCC (Upper Continental Crust), NASC (North American Shale Composite) and PAAS (Post-Archean Australian Shale). Major elements are expressed in %

	S1 (9)	S1(10)	S1(10-13)	S1(13-14)	S1(14)	S1(15)	S1(16)	Av.	UCC	NASC	PAAS
SiO_2	11.85	9.42	22.4	6.26	8.92	3.09	11.3	10.46	65.89	64.8	62.8
Fe_2O_3	7.32	7.28	15.77	4.5	8.65	7.66	4.75	7.99	4.49	5.65	7.22
Al_2O_3	8	6.4	7.15	7.43	1.81	0.53	2.25	4.8	15.17	16.9	18.9
CaO	50.4	54.45	40.6	71.05	32.4	69.9	27.5	49.47	4.19	3.63	1.3
MgO	1.89	1.74	4.51	1.09	2.82	1.06	1.18	2.04	2.2	2.86	2.2
K2O	1.14	0.52	1.05	0.38	0.32	0.12	0.32	3.85	3.39	3.97	3.7
Na_2O	2.55	2.07	3.95	1.52	4.06	2.45	2.29	2.7	3.89	1.14	1.2
TiO_2	0.23	0.2	0.17	0.18	0.27	0.28	0.2	0.25	0.5	0.7	1
P_2O_5	1.18	1.02	1.92	0.83	1.33	0.97	0.95	1.17	0.2	0.13	0.16
MnO	0 .095	0.076	0.157	0.077	0.087	0.116	0.058	0.095	0.069	0.05	0.08

Table 3. Concentrations of trace elements in the black shale form the Ama Fatma site along with the corresponding averaged values in UCC (Upper Continental Crust), NASC (North American Shale Composite) and PAAS (Post-Archean Australian Shale). Trace elements are in ppm. n.d.means not determined

	S1(9)	S1(10)	S1(10-13)	S1(13-14)	S1(14)	S1(15)	S1(16)	Av.	UCC	NASC	PAAS
Li	27.17	18.11	62.4	9.82	31.14	15.52	8.88	24.72	20	n.d.	n.d.
Be	7.19	17.44	61.64	22.15	582.02	4.41	3.88	179.1	3	n.d.	n.d.
V	246.65	276.28	425.52	181.37	1010.75	496.73	382.59	431.41	107	130	150
Cr	95.81	78.09	130.29	37.81	143.57	75.61	71.63	90.4	85	68.42	68.42
Co	85.15	74.94	164.68	103.19	119.26	37.31	78.83	663.36	17	25.7	23
Ni	142.6	95.37	223.5	56.41	285.04	140.27	144.29	155.35	44	58	55
Cu	27.82	24.73	32.8	18.65	56.67	33.51	30.61	32.11	25	n.d.	50
Zn	119.51	163.77	151.63	83.72	273.88	206.26	209.84	172.66	71	n.d.	85
Ga	6.29	6.22	8.03	4.73	4.59	6.5	5.46	5.97	17	n.d	20
Rb	19.46	12.72	24.9	6.44	8.08	25.69	13.67	15.85	112	125	160
Sr	516.95	588.54	448.87	556.65	664.49	246.68	463.29	497.92	350	142	200
Zr	31.85	27.47	63.63	19.42	34.41	38.26	32.18	35.32	190	200	210
Nb	4.92	4.47	6.53	3.67	2.8	6.9	4.33	4.8	12	13	19
Mo	65.69	57.65	47.6	50.92	52.53	78.2	78.34	61.56	1.5	n.d.	1
Cd	0.56	0.84	1.23	0	1.05	2.61	0.83	1.19	0.098	n.d.	n.d.
In	0.08	0.11	0	0.1	0	0.09	0.09	0.09	0.05	n.d.	n.d.
Sb	1.3	1.28	1.55	0.79	1.14	2.72	2.41	1.6	0.2	2.09	n.d
Ba	106.47	98.72	129.46	180.52	81.36	100.81	106.9	114.89	550	636	650
Au	2.2	0.79	1.29	0	0.14	0.05	0.43	0.82	0	n.d.	n.d.
Pb	70.04	37.31	26.25	96.5	39.43	18.5	50.17	48.31	17	n.d.	20
Bi	569	551.57	935.02	316.61	456.79	551.41	723.15	586.22	0.13	n.d.	n.d.
Th	2.65	2.4	4.48	1.29	1.55	2.35	2.65	2.48	10.7	12.3	14.6

3.2. Major Elements Geochemistry

Major elements were analyzed in our sample in order to use them in conjunction with the mineralogical data to establish the element/mineral association. Although elements associations could vary from one sample to another, a correlation analysis would indicate the general trends (Fu et al. 2010a). Major elements concentrations are presented in Table 2. CaO, whose concentration varied between 27.5 – 71.05%, was the most abundant in our samples, followed in importance by silicon and iron oxides, SiO_2 (3,09-22,4%) and Fe_2O_3 (4,50-15,77%), while Al_2O_3 (0,53 - 8%), Na_2O (1,52-4,06%) and MgO (1,09-4,51%) were less abundant. Other elements such as P_2O_5, K_2O, TiO_2 and MnO were present in weak concentrations, often less than 1%. The average concentrations of Al_2O_3, K_2O, TiO_2 and MgO were similar to those reported for the widely used geochemical standards; the Upper Continental Crust (UCC; Taylor and McLennan 1985), Post Archean Australian Shale (PAAS; Taylor and McLennan 1985) and North American Shale Composite (NASC; Gromet et al. 1984). On the other hand, CaO, Fe_2O_3, P_2O_5 and MnO exhibited higher concentrations compared to these standards, while SiO_2 was much lower. Exceptionally, CaO (27.5 – 71.05%), higher by one order of magnitude than the geochemical standards, indicated a predominance of carbonates in the sedimentary environment

of the Ama Fatma site, which should be associated to the abundant bivalve and gastropods fossilized remains. In addition, carbonate precipitation occurs normally in open marine environments characterized by weak clastic inputs in the water. Therefore, the high carbonate content in the black shale of Ama Fatma reveals that deposition occurred in an open marine setting, as reported in previous research for similar environment (Armenteros and Huerta 2006).

Pearson correlations among major elements are given in Table 4. Fe_2O_3, Al_2O_3, MgO, Na_2O, TiO_2, P_2O_5 and MnO were found to be negatively correlated to TOC and CaO. The degrees of correlation vary from one element to another and are, in general, moderate to weak. This suggests that these oxides are not associated to organic matter and carbonate contents, but rather to the terrigenous fractions and associated minerals. On the other hand, SiO_2 is positively well correlated to Fe_2O_3 (r = 0, 77), MgO (r = 0, 85), Na_2O (r = 0, 57), TiO_2 (r = 0, 69), P_2O_5 (r = 0, 86) and MnO (r = 0, 56), indicating that these elements are of terrestrial origin and have been probably transported as detrital components. Silicium found in black shale is, in general, of terrestrial origin (Sari et al 2012). The relatively low contents of Al_2O_3 and SiO_2 should be attributed to the low quantity of clay material in our samples. The positive correlation among Al_2O_3, K_2O and SiO_2 indicates that these elements are associated to the clay fraction, and the samples are essentially composed of illite.

The non-significant negative correlation between P_2O_5 and TOC reveals that the phosphate is not associated to the organic phase. It is well known that this element is often confined in the apatite (Kasper-Zubillaga et al. 2008; Fu et al. 2010b), and cannot precipitate directly with the inorganic component in seawater and, therefore, phosphorous has been incorporated to the sedimentary shale along with the terrigenous substances (Mu 1999). In addition, the strong correlations among Mn, Fe and P are indicative of the presence of H_2S which promote the precipitation of these elements as oxides (Kholodov 2001). This could be behind their relative high concentrations compared to UCC, PAAS and NASC.

3.3. Uraniumand Thorium

U and Th concentrations found in the black shale from Ama Fatma were ranging from 4.09 to 17.84 ppm and from 1.29 to 4.48 ppm with depth averaged values of 13.2 ppm and 2.48 ppm, respectively. U levels are much higher than those reported for the geological standards (UCC, PAAS and NASC) while Th levels are lower. This ultimate was found to be significantly and positively correlated to SiO_2, Fe_2O_3, MgO, K_2O, TiO_2, P_2O_5, and MnO, and not correlated to TOC and CaO indicating that thorium is pre-dominantly of detrital origin. The weak correlation between U and TOC, and the non-correlation with SiO_2 and Fe_2O_3 might be due to the relatively high content of OM which could influence the oxidation state of U, and consequently its solubility/mobility. In addition, organic matter may possibly compete with U in the sorption processes onto mineral surfaces, such as Fe- and Si- oxides and hydroxides (Cumberland et al. 2016).

3.4. Trace Elements Geochemistry and Enrichment

From trace elements abundances given in Table 3, Li, Cr, Cu, In, Sb were found to be of the same range of concentrations of the averages reported for geological standards (UCC, PAAS and NASC), while elements such as Ga, Rb, Zr, Nb, Ba and Th are lower. In contrast, Be, V, Co, Ni, Zn, Sr, Mo, Cd, Pb, Bi and U presented concentrations higher, to much higher, than the standards. On the other hand, all trace elements, except for Mo and Sb, did not appear to be associated to organic matter as can be seen in the correlation table. The negative correlations of some heavy metal elements with CaO could be attributed to the adsorption mainly on clay and/or MnO minerals. Secondly, the heavy metals may enter the calcium lattice defects and, therefore, constitute metal carbonate (Aziz HA et al. 2008).

Element enrichments in our black shale samples were estimated by using the Enrichment Factor (EF) defined as follows (Brumsack 2006):

$$EF = \left(\frac{X}{Al}\right)_{sample} / \left(\frac{X}{Al}\right)_{PAAS} \quad (1)$$

Where X and Al are the element and aluminium concentrations. Al has been used as normalizing element to compensate for grain size and mineralogical variability, since it represents alumino-silicates (Luoma and Rainbow 2008). In Table 5, EFs calculated from equation (1) are presented. The studied trace elements were found to be classified in five categories according to the enrichment levels established through the averaged EF throughout the vertical section (Sutherland 2000):

- EF<2, weakly enriched: Ba
- 2<EF<5, moderately enriched: Rb, Zr
- 5<EF<20, significantly enriched: Cu, Ga, Nb, Th, Cr, Sr
- 20<EF<40, highly enriched: Pb, Zn, Ni, Co, V
- EF>40, extremely enriched: U, Mo

The depth-averaged EFs were in the order Ba<Rb<Zr <Cu<Ga<Nb<Th<Cr<Sr<Pb<Zn<Ni<Co<V<U<Mo. Mo showed the highest enrichment because of its links with pyrite and sulfur-rich organic matter (Tribovillard et al. 2004). Therefore, the extreme enrichment in Mo (EF: 793.47) and U (EF: 94.16) and high enrichment in Co, Ni, V, Zn and Pb (EF: 23, 57-32, 70) in our samples suggested that the Ama Fatma bituminous shale was deposited under euxinic conditions.

V and Ni seem to be highly enriched in our samples. Such enrichment occurs usually in bitumen that is associated with type I and II kerogen as suggested by Lewan and Maynard (1982). Therefore, the organic matter contained in the Ama Fatma shale is associated with type II kerogen, in agreement with previous studies carried out on samples from the same site (El Albani 1995; El Batal 2014).

Table 4. Pearson's correlations among major and trace elements

	TOC	SiO2	Fe2O3	Al2O3	CaO	MgO	K2O	Na2O	TiO2	P2O5	MnO	Li	Be	V	Cr	Co	Ni	Cu	Zn	Ga	Rb	Sr	Zr	Nb	Mo	Cd	In	Sb	Ba	Au	Pb	Bi	Th	U
TOC	1,00	-0,04	-0,42	-0,54	-0,58	-0,42	-0,29	-0,21	-0,30	-0,33	-0,49	-0,43	-0,38	-0,08	-0,24	-0,43	-0,07	-0,04	0,28	-0,16	0,02	-0,47	-0,11	-0,04	0,91	0,06	0,26	0,89	-0,20	-0,08	-0,01	0,28	0,06	0,35
SiO2		1,00	0,78	0,47	-0,55	0,85	0,76	0,57	0,70	0,86	0,56	0,84	0,61	-0,05	0,55	0,81	0,42	0,04	-0,14	0,65	0,33	0,14	0,77	0,24	-0,44	-0,19	-0,59	-0,16	0,04	0,59	-0,19	0,82	0,85	0,00
Fe2O3			1,00	0,19	-0,25	0,94	0,55	0,78	0,97	0,96	0,90	0,97	0,78	0,25	0,73	0,69	0,61	0,30	0,09	0,77	0,59	-0,12	0,94	0,51	-0,48	0,32	-0,76	-0,03	-0,12	0,37	-0,57	0,72	0,80	0,08
Al2O3				1,00	0,21	0,27	0,77	-0,20	0,02	0,23	0,16	0,31	-0,04	-0,65	-0,14	0,45	-0,37	-0,60	-0,85	0,28	-0,07	0,36	0,00	-0,03	-0,59	-0,68	0,12	-0,69	0,55	0,63	0,54	0,05	0,25	-0,55
CaO					1,00	-0,45	-0,19	-0,60	-0,23	-0,44	0,10	-0,33	-0,50	-0,48	-0,63	-0,43	-0,68	-0,56	-0,57	0,02	0,11	-0,37	-0,35	0,30	0,00	0,13	0,55	-0,08	0,50	-0,20	0,25	-0,52	-0,32	-0,60
MgO						1,00	0,60	0,85	0,87	0,98	0,74	0,98	0,90	0,35	0,82	0,87	0,71	0,40	0,12	0,56	0,31	0,20	0,84	0,20	-0,64	0,04	-0,86	-0,26	-0,11	0,38	-0,39	0,64	0,69	0,09
K2O							1,00	0,29	0,43	0,63	0,47	0,67	0,26	-0,33	0,36	0,55	0,14	-0,20	-0,49	0,58	0,35	0,17	0,45	0,23	-0,39	-0,34	-0,28	-0,38	0,10	0,93	0,13	0,48	0,63	-0,04
Na2O								1,00	0,78	0,85	0,59	0,81	0,93	0,76	0,97	0,64	0,97	0,81	0,57	0,30	0,27	0,15	0,74	0,08	-0,36	0,30	-0,97	-0,02	-0,47	0,17	-0,56	0,49	0,45	0,48
TiO2									1,00	0,92	0,94	0,92	0,77	0,31	0,69	0,62	0,64	0,35	0,16	0,75	0,66	-0,30	0,97	0,60	-0,33	0,45	-0,78	0,15	-0,10	0,25	-0,61	0,73	0,78	0,08
P2O5										1,00	0,80	0,99	0,85	0,31	0,81	0,81	0,71	0,38	0,12	0,66	0,46	0,05	0,91	0,34	-0,52	0,14	-0,85	-0,12	-0,14	0,44	-0,45	0,72	0,77	0,14
MnO											1,00	0,84	0,58	0,10	0,51	0,48	0,41	0,13	-0,08	0,80	0,76	-0,43	0,88	0,73	-0,32	0,47	-0,59	0,11	0,05	0,31	-0,50	0,58	0,72	-0,09
Li												1,00	0,83	0,26	0,78	0,80	0,65	0,32	0,03	0,68	0,47	0,04	0,89	0,36	-0,57	0,13	-0,82	-0,19	-0,08	0,47	-0,41	0,67	0,75	0,07
Be													1,00	0,68	0,86	0,82	0,86	0,69	0,40	0,22	0,06	0,30	0,69	-0,05	-0,64	0,09	-0,97	-0,26	-0,17	0,02	-0,38	0,39	0,37	0,16
V														1,00	0,74	0,20	0,86	0,99	0,88	-0,27	-0,13	0,22	0,24	-0,28	-0,11	0,37	-0,72	0,06	-0,60	-0,35	-0,48	-0,03	-0,17	0,59
Cr															1,00	0,57	0,95	0,81	0,57	0,29	0,24	0,25	0,67	0,01	-0,35	0,25	-0,90	-0,09	-0,59	0,30	-0,55	0,45	0,42	0,59
Co																1,00	0,51	0,23	-0,10	0,24	-0,08	0,44	0,57	-0,13	-0,81	-0,38	-0,76	-0,53	0,27	0,24	0,05	0,42	0,45	-0,24
Ni																	1,00	0,92	0,71	0,12	0,16	0,18	0,61	-0,06	-0,22	0,31	-0,93	0,04	-0,57	0,07	-0,53	0,39	0,29	0,60
Cu																		1,00	0,87	-0,21	-0,06	0,23	0,29	-0,26	-0,09	0,35	-0,75	0,07	-0,67	-0,20	-0,48	0,05	-0,08	0,68
Zn																			1,00	-0,21	-0,02	0,02	0,18	-0,16	0,27	0,53	-0,45	0,42	-0,79	-0,39	-0,65	0,12	-0,09	0,78
Ga																				1,00	0,87	-0,52	0,81	0,86	-0,03	0,42	-0,22	0,31	-0,07	0,55	-0,55	0,81	0,92	0,02
Rb																					1,00	-0,80	0,72	0,96	0,34	0,71	-0,16	0,61	-0,22	0,42	-0,62	0,67	0,75	0,21
Sr																						1,00	-0,35	-0,87	-0,63	-0,75	-0,20	-0,83	-0,01	0,07	0,43	-0,34	-0,36	0,01
Zr																							1,00	0,64	-0,19	0,46	-0,71	0,28	-0,17	0,32	-0,65	0,86	0,88	0,17
Nb																								1,00	0,31	0,69	0,00	0,61	-0,01	0,26	-0,55	0,60	0,70	-0,03
Mo																									1,00	0,48	0,49	0,85	-0,38	-0,08	-0,22	0,06	-0,07	0,45
Cd																										1,00	-0,16	0,77	-0,51	-0,22	-0,84	0,29	0,26	0,43
In																											1,00	0,15	0,24	-0,09	0,39	-0,42	-0,39	-0,27
Sb																												1,00	-0,39	-0,19	-0,60	0,42	0,29	0,42
Ba																													1,00	-0,14	0,68	-0,21	-0,09	-0,97
Au																														1,00	0,07	0,44	0,57	0,20
Pb																															1,00	-0,57	-0,51	-0,58
Bi																																1,00	0,96	0,25
Th																																	1,00	0,10
U																																		1,00

Table 5. Mean enrichment factor (EF) of selected trace elements in the Ama Fatma black shale section. EF = (X/Al) sample/(X/Al) PAAS

PAAS(EF)	S1(9)	S1(10)	S1(10-13)	S1(13-14)	S1(14)	S1(15)	S1(16)	average
Si	0.45	0.44	0.94	0.25	1.48	1.74	1.51	0.97
Fe	2.39	2.98	5.78	1.59	12,51	37,58	5,53	9.76
Ca	91.59	123.69	82.55	139.03	260.26	1903.20	177.69	396.86
Mg	2.03	2.33	5.41	1.26	13.38	17.17	4.51	6.59
K	0.73	0.42	0.75	0.26	0.91	1.12	0.75	0.70
Na	5.03	5.12	8.71	3.23	35.36	72.55	16.09	20.87
Ti	0.55	0.61	1.15	0.45	2.73	10.35	1.65	2.50
P	17.37	18.81	31.72	13.17	87.04	213.88	49.70	61.67
Mn	2.83	2.83	5.21	2.48	11.40	51.49	6.18	11.78
V	3.88	5.44	7.50	3.08	70.36	117.21	21.43	32.70
Cr	3.31	3.37	16.44	1.41	21.91	39.12	8.79	13.48
Co	8.75	9.62	48.90	11.41	54.15	57.42	28.79	31.29
Ni	6.13	5.12	20.45	2.61	54.12	90.27	22.04	28.68
Cu	1.31	1.46	22.50	0.95	11.84	23.72	5.14	9.56
Zn	3.32	5.69	13.23	2.51	33.65	85.89	20.74	23.57
Ga	0.74	0.92	56.24	0.60	2.40	11.50	2.29	10.67
Rb	0.29	0.23	7.03	0.10	0.53	5.68	0.72	2.08
Sr	6.11	8.69	5.62	7.08	34.69	43.66	19.46	17.90
Zr	0.36	0.39	5.36	0.24	1.71	6.45	1.29	2.25
Nb	0.61	0.69	59.20	0.49	1.54	12.85	1.91	11.04
Mo	155.19	170.25	1124.81	129.53	548.54	2767.94	658.06	793.48
Ba	0.39	0.45	1.73	0.71	1.31	5.49	1.38	1.64
Pb	8.27	5.51	56.24	12.27	20.59	32.74	21.07	22.39
Th	0.43	0.49	77.04	0.22	1.11	5.70	1.52	12.36
U	11.76	13.08	362.84	3.36	60.09	165.56	42.49	94.17

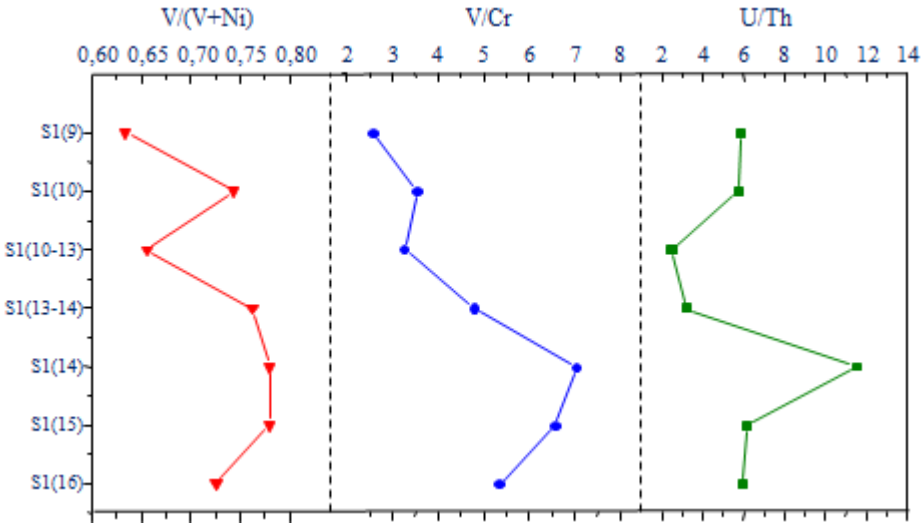

Figure 3. Vertical profiles of V/(V+Ni), V/Cr and U/Th in black shale form the Ama Fatma site

3.5. Redox Conditions Reconstruction

Trace elements ratios are widely used as proxies for establishing the redox conditions of the depositional environment in old and modern sedimentary systems (Calvert and Pedersen 1993; Jones and Manning 1994; Wignall 1994; Crusius et al. 1996; Dean et al. 1997, 1999; Yarincik et al. 2000; Morford et al. 2001; Pailler et al. 2002). Indeed, previous studies have used ratios such as V/(V + Ni), V/Cr and U/Th to reconstruct redox conditions under which the geological formations occurred (Hatch and Leventhal 1992; Jones and Manning 1994; Rimmer et al. 2004). In Figure 3, the vertical profiles of the above mentioned ratios are plotted.

According to Lewanand Hatch and Leventhal (1992), V/(V+Ni) ratios greater than 0.84 are indicative of euxinic conditions, while ratios ranging from 0.54 to 0.82 and from 0.46 to 0.60 are typical of anoxic and dysoxic conditions, respectively. V/(V+Ni) ratios between 0.63 and 0.78 were obtained for our black shale samples, pointing toward anoxic conditions during the deposition.

V/Cr ratio has also been used as indicator of redox conditions changes in deposition environments. Vanadium, which is initially incorporated in tetrapyrrole structures, is preferably accumulated in reducing conditions (Calvert and Piper 1984; Tribovillard et al. 2006; Soua 2010). This element can also be adsorbed on clay minerals during burial (Breitand Wanty 1991), while chromium is associated to the detrital and is not biased by the prevailing oxydoreduction conditions (Dill 1986). Ratios of V/Cr greater than 2 are indicative of anoxic condition, while values lesser than 2 suggest oxidative conditions. The ratios found for our samples were all ranging from 2.57 and 7.04 revealing anoxic depositional conditions. The lowest value was recorded at the upper layer S1(9) followed by an increase to a maximum at S1(14) and then a decrease. Such substantial variability throughout the shale rock column should be attributable to changes in redox potential during deposition.

U/Th ratio has also been used as excellent indicator of redox conditions due to different behavior of U and Th in terms of solubility in aqueous suspensions (Dill 1986; Jones and Manning 1994; Rimmer et al. 2004). Indeed, U(IV), in oxygen depleted environments, is reduced to its insoluble form U(IV) which is predominantly adsorbed onto particles (Algeo and Maynard 2004; Tribovillard et al. 2006). In contrast, Th is known to be a high reactive-particle element and, therefore, remains practically associated to clay minerals, insoluble debris or heavy minerals (Anderson et al. 1983). Consequently, high U/Th ratios (>1.25) are indicative of anoxic conditions, while values lesser than 0.75 are characteristic of oxic environments (Jones and Manning 1994). The U/Th values found in our samples were all ranging from 2.47 to 11.51, revealing that the corresponding black shale were deposited while anoxic conditions were prevailing, being in good agreement with the previous results using V/(V+Ni) and V/Cr as proxies of redox conditions.

4. Conclusions

In the present work, the geochemical characterization of the black shale from the Ama Fatma coastal site was investigated as a preliminary step for the use of this geological matrix in the storage of radioactive wastes. The results showed that:

1. Particle size distribution in black shale are dominated by sand followed by silt and then clays, giving our black shale a sandy loam texture;
2. The mineralogical composition of Ama Fatma black shale is dominated by calcite with a low fraction of dolomite, Quartz, clays, halite, fluorapatite and pyrite;
3. Major element distributions showed higher concentration of CaO followed by SiO_2 and Fe_2O_3, while the other elements were less abundant;
4. The high carbonate content in the Ama Fatma black shale reveals that deposition occurred in an open marine setting;
5. The correlation among major elements of our samples indicates that these oxides are associated to the terrigenous fractions and associated minerals;
6. U and Th concentrations were found to be controlled by organic matter content and detrital component;
7. Trace elements distribution show a high enrichment in Mo, U, Co, Ni, V, Zn and Pb indicating that the Ama Fatma bituminous shale was deposited under euxinic conditions;
8. The high enrichment in V and Ni suggested that our bituminous shale are associated with type I and II kerogen;
9. Trace elements ratios revealed an anoxic condition deposition of our studied oil shale.

ACKNOWLEDGEMENTS

This work has been carried out within the framework of the UMR between the University Hassan 2 - Casablanca and the National Center for Energy, Nuclear Science and Technology, and in the framework of the collaboration held between the Faculty of Sciences-Rabat and the University of Seville - Spain.

REFERENCES

[1] Alaoui-Sosse A, Gaboriaud F, Vantelon J P, Halim M, Ziyad M (1988) Degradation thermique des schistes bitumineux de Timahdit. Etude sur la formation des principaux gaz de pyrolyse. J ChimPhys 85(1), 103-111.

[2] Algeo TJ, Maynard JB (2004) Trace-element behavior and redox facies in core shales of Upper Pennsylvanian Kansas-type cyclothems. Chem Geol 206, 289–318.

[3] Ambles A, Dupas G, Jacquesy J C, Vitorovic D (1988) Chemical characterization of the kerogen from Moroccan Timahdit black shale by analysis of oxidation products. Org Geochem, Vol. 13, pp. 1031-1038.

[4] Anderson RF, Bacon MP, Brewer PG (1983) Removal of ^{230}Th and ^{231}Pa at ocean margins. Earth Planet SciLett. 66, 73–90.

[5] Armenteros I, Huerta P (2006) The Role of Clastic Sediment Influx in the Formation of Calcrete and Palustrine Facies: A Response to Paleographic and Climatic Conditions in the Southeastern Tertiary Duero Basin (Northern Spain). Geological Society of America Special Papers, vol. 416, pp. 119–132.

[6] Aziz HA, Adlan MN, Ariffin KS (2008) Heavy metals (Cd, Pb, Zn, Ni, Cu and Cr(III)) removal from water in Malaysia: post treatment by high quality limestone. Bioresour Technol. 99(6), 1578–83.

[7] Bekri O, Ziyad M (1991) Abstract presented at Black shale Symposium, Lexington, Kentucky, U.S.A.

[8] Breit GN, Wanty RB (1991) Vanadium accumulation in carbonaceous rocks: a review of geochemical controls during deposition and diagenesis. ChemGeol, 91 (2), 83–97.

[9] Brumsack HJ (2006) The trace metal content of recent organic carbon-rich sediments: implications for Cretaceous black shale formation. Palaeogeogr Palaeoclimatol Palaeoecol, 232, 344–361.

[10] Calvert SE, Piper DZ (1984) Geochemistry of ferromanganese nodules from DOMES site a, Northern Equatorial Pacific: multiple diagenetic metal sources in the deep sea. Geochim Cosmochim Acta 48 (10), 1913–1928.

[11] Calvert SE, Pedersen TF (1993) Geochemistry of recent oxic and anoxic marine sediments: implications for the geological record. Mar Geol, 113 (1–2), 67–88.

[12] Crusius J, Calvert S, Pedersen T, Sage D (1996) Rhenium and molybdenum enrichments in sediments as indicators of oxic, suboxic and sulfidic conditions of deposition. Earth Planet SciLett145, 65–78.

[13] Cumberland S, Douglas G, Grice K, Moreau J (2016) Uranium mobility in organic matter-rich sediments: A review of geological and geochemical processes. Earth-Science Reviews, V 159, 160–185.

[14] Dean WE, Gardner JV, Piper DZ (1997) Inorganic geochemical indicators of glacial–interglacial changes in productivity and anoxia of the California continental margin. Geochim Cosmochim Acta 61, 4507– 4518.

[15] Dean WE, Piper DZ, Peterson LC (1999) Molybdenum accumulation in Cariaco basin sediment over the past 24 ky: a record of water-column anoxia and climate. Geology 27,507–510.

[16] Dill H (1986) Metallogenesis of early Paleozoic graptolite shales from the Graefenthal Horst (northern Bavaria-Federal Republic of Germany). Econ Geol 81 (4), 889–903.

[17] Dyni J R (2006) Black shale developments in the United States .Oil Shale, 23(2), 97–98.

[18] Einsele G, Wiedmann J (1982) Turonian Black Shales in the Moroccan coastal basins: First upwelling in the Atlantic Ocean. In U.von Rad, K. Hinz, M. Sarnthein and E. Seibold (Eds.), Geology of the Northwest African Continental margin. Springer- Verlag, 396-414.

[19] EL Albani A (1995). Les formations du crétacé supérieur du bassin de Tarfaya (Maroc méridional): Sédimentologie et géochimie. Ph. Dthesis, Lille Univ, France.

[20] El Batal Y (2014) Le potentiel pétrolier du bassin méso-cénozoïque Tarfaya-Boujdour: Caractérisation sédimentologique, lithostratigraphique, géophysique et géochimique de la roche mère d'âge crétacé supérieur. Ph. Dthesis, Casablanca Univ, Morocoo.

[21] Fu XG, Wang J, Zeng YH, Tan FW, Feng XL (2010a) REE geochemistry of marine oil shale from the Changshe Mountain area, northern Tibet, China Int J Coal Geol -81,191–199.

[22] Fu X, Wang J, Zeng Y, Tan F, He J (2010b) Geochemistry and origin of rare earth elements (REEs) in the Shengli River oil shale, northern Tibet, China. Chem Erde-Geochem, 71(1), 21–30.

[23] Galindo C, Mougin L, Fakhi S, Nourreddine A, Lamghari A, Hannache H (2007) Distribution of naturally occurring radionuclides (U, Th) in Timahdit black shale (Morocco). Journal of Environmental Radioactivity, 92 (2007), 41-54.

[24] Gebhardt H, Zorn I (2008) Cenomanian ostracods of the Tarfaya upwelling region (Morocco) as palaeo environmental indicators. Revue de Micropaléontologie, volume 51, Issue 4, pages 273-286.

[25] Gromet LP, Dymek RF, Haskin L A, Korotev RL (1984) The North American shale composite: Its compilation, major and trace element characteristics. Geochimica et cosmochimica Acta Vol. 48. pp. 2469-2482.

[26] Hatch JR, Leventhal JS (1992) Relationship between inferred redox potential of the depositional environment and geochemistry of the Upper Pennsylvanian (Missourian) Stark Shale Member of the Dennis Limestone, Wabaunsee County, Kansas, USA. ChemGeol 99 (1–3), 65–82.

[27] Jones B, Manning DAC (1994) Comparison of geochemical indices used for the interpretation of palaeoredox conditions in ancient mudstones. Chem Geol 111(1–4), 111–129.

[28] Kasper-Zubillaga J J, Acevedo-Vargas B, Morton-Bermea OM, Ortiz-Zamora G (2008) Rare earth elements of the Altar Desert dune and coastal sands, Northwestern Mexico. ChemErde-Geochem, 68, 45–59.

[29] Kholodov VN (2001) The Role of H2S-Contaminated Basins in Sedimentary Ore Formation. Lithology and Mineral Resources. Vol. 37, No. 5, pp. 393–411.

[30] Khouya El (2002) Elaboration de nouveaux adsorbants à partir des schistes bitumineux Marocains: Application au traitement des effluents faiblement contaminés par des radioéléments. Ph.D thesis, Casablanca Univ, Morocoo.

[31] Kolonica S, Sinninghe Damsté JS, Böttcher ME, Kuypers MMM, WKuhnt, Beckmann B, Scheeder G, Wagner T (2002) Geochemical characterization of cenomanian/Turonian black shales from the Tarfaya basin (SW Morocco). Journal of Petroleum Geology.25, 325–350.

[32] Lewan MD, Maynard JB (1982) Factors controlling enrichment of vanadium and nickel in the bitumen of organic sedimentary rocks. Geochim Cosmochim Acta 46 (12), 2547–2560.

[33] Luoma SN, Rainbow PS (2008) Metal contamination in aquatic environment. Science and lateral management, Cambridge. 573p.

[34] Morford JL, Russell AD, Emerson S (2001) Trace metal evidence for changes in the redox environment associated with the transition from terrigenous clay to diatomaceous sediment, Saanlich Inlet, BC. Mar. Geol. 174, 355– 369.

[35] Mu BL (1999) Element geochemistry. Beijing: Tsinghua University Press, p. 206–10 (in Chinese).

[36] Neuzil CE (2014) Shale: an overlooked option for US nuclear waste disposal. Bulletin of the Atomic Scientists.

[37] Nuttall HE, Guo T M, Schrader S, Thakur DS (1983) Pyrolysis kinetics of several key-world oil shales. In Geochemistry and Chemistry of Oil Shales, pp 270-300.ACS Symposium Series 230.

[38] Pailler D, Bard E, Rostek F, Zheng Y, Mortlock R, Van Geen A (2002) Burial of redox-sensitive metals and organic matter in the equatorial Indian Ocean linked to precession. Geochim Cosmochim Acta 66, 849– 865.

[39] Qian JL (2006) China's oil business is going ahead .Oil Shale.

23(4), 295.

[40] Rimmer SM, Thompson JA, Goodnight SA, Robl TL (2004) Multiple controls on the preservation of organic matter in Devonian–Mississippian marine black shales: geochemical and petrographic evidence. Palaeogeogr Palaeoclimatol Palaeoecol, 215 (1–2), 125–154.

[41] Sari A, Derya K (2012) An approach to provenance, tectonic and redox conditions of Jurassic-cretaceous akkuyuformation, central Taurids, Turkey. Mineral Res. Expl. Bull, 144, 51-74.

[42] Saoiabi A, Doukkali A, Hamad M, Zrineh A (2001) Schistes bitumineux de Timahdit (Maroc): composition et propriétés physicochimiques. Chemistry 4, 351–360.

[43] Soua M (2010) Productivity and bottom water redox conditions at the Cenomanian–Turonian Oceanic Anoxic Event in the southern Tethyanmargin, Tunisia. Revue Méditerranéenne de l'Environnement, 4, 653–664.

[44] Sutherland RA (2000) Bed sediment-associated trace metals in an urban stream, Oahu. Hawaii. Environmental Geology. 39: 611–627.

[45] Hansen FD, Hardin EL, Rechard RP, Freeze GA, Sassani DC, Brady PV, Stone CM, Martinez MJ, Holland JF, Dewers T, Gaither KN, Sobolik SR, Cygan RT (2010) Shale Disposal of U.S. High-Level Radioactive Waste. Rapport Sandia National Laboratories.

[46] Taylor SR, McLennan SM (1985) The Continental Crust: Its Composition and Evolution. Blackwell, Oxford, pp. 28–29.

[47] Tribovillard N, Riboulleau A, Lyons T, Baudin F (2004) Enhanced trapping of molybdenum by sulfurized marine organic matter of marine origin in Mesozoic limestones and shales. ChemGeol213, 385–401.

[48] Tribovillard N, Algeo TJ, Lyons TW, Riboulleau A (2006) Trace metal as paleoredox and paleoproductivity proxies: an update. ChemGeol 232, 12–32.

[49] Wignall PB (1994) Black shales. Clarendon Press, Oxford. 127 pp.

[50] Yarincik KM, Murray RW, Lyons TW, Peterson LC, Haug GH (2000) Oxygenation history of bottom waters in the Cariaco Basin, Venezuela, over the past 578,000 years: results from redox-sensitive metals (Mo, V, Mn, and Fe). Paleoceanography 15, 593– 604.